Research Square

Preprints are preliminary reports that have not undergone peer review.
They should not be considered conclusive, used to inform clinical practice,
or referenced by the media as validated information.

Aging-associated cutaneous IgM autoreactivity identifies acquired anti-collagen XVII IgM alongside lifelong anti-collagen VII natural IgM in mice

Chihiro Shiiya
Hokkaido University
Ken Muramatsu
k-muramatsu@med.hokudai.ac.jp

Hokkaido University
Norihiro Yoshimoto
Hokkaido University
Sho Katayama
Hokkaido University
Takuya Kawamura
Hokkaido University
Shoko Mai
Hokkaido University
Yosuke Mai
Hokkaido University
Takamasa Ito
Hokkaido University
Kentaro Izumi
Hokkaido University
Ken Natsuga
Hokkaido University
Hiroaki Iwata
Gifu University
Hiroyuki Kitahata
Chiba University
Yoichiro Fujioka
Hokkaido University
Yusuke Ohba
Hokkaido University
Kentaro Saito

Hokkaido University

Utano Tomaru

Hokkaido University Hospital

Yoshinori Hasegawa

Kazusa DNA Research Institute

Hideyuki Ujiie

Hokkaido University

Article

Keywords:

Posted Date: November 2nd, 2026

DOI: https://doi.org/10.21203/rs.3.rs-10549604/v1

License: This work is licensed under a Creative Commons Attribution 4.0 International License.
Read Full License

Additional Declarations: No competing interests reported.

---

npj Aging

Article

Aging-associated cutaneous IgM autoreactivity identifies acquired anti-collagen XVII IgM alongside lifelong anti-collagen VII natural IgM in mice

Chihiro Shiiya[1], Ken Muramatsu[1], Norihiro Yoshimoto[1], Sho Katayama[1], Takuya Kawamura[1], Shoko Mai[1], Yosuke Mai[1], Takamasa Ito[1], Kentaro Izumi[1], Ken Natsuga[1], Hiroaki Iwata[2], Hiroyuki Kitahata[3], Yoichiro Fujioka[4], Yusuke Ohba[4], Kentaro Saito[5], Utano Tomaru[6], Yoshinori Hasegawa[7], Hideyuki Ujiie[1]

1 Department of Dermatology, Faculty of Medicine and Graduate School of Medicine, Hokkaido University, Sapporo, Japan

2 Department of Dermatology, Graduate School of Medicine, Gifu University, Gifu, Japan

3 Department of Physics, Graduate School of Science, Chiba University, Chiba, Japan

4 Department of Cell Physiology, Faculty of Medicine, Hokkaido University, Sapporo, Japan

5 Department of Medical Laboratory Science, Faculty of Health Sciences, Hokkaido University, Sapporo, Japan.

6 Department of Surgical Pathology, Hokkaido University Hospital, Sapporo, Japan

7 Department of Applied Genomics, Kazusa DNA Research Institute, Kisarazu, Japan

Abbreviations

AIRE: autoimmune regulator

BP: bullous pemphigoid

B6J: C57BL/6J

COL17: type XVII collagen

COL7: type VII collagen

DEJ: dermal-epidermal junction

DIF: direct immunofluorescence

DPP-4: Dipeptidyl peptidase-4

EBA: epidermolysis bullosa acquisita

IIF: indirect immunofluorescence

mTECs: medullary thymic epithelial cells

NC: negative control

PC: positive control

PD-1: programmed cell death 1

RA: rheumatoid arthritis

SLE: systemic lupus erythematosus

Treg: regulatory T cells

WB: western blotting

Corresponding author:

Ken Muramatsu, M.D., Ph.D.

Department of Dermatology, Faculty of Medicine and Graduate School of Medicine, Hokkaido University, North 15 West 7, Kita-ku, Sapporo 060-8638, Japan

Tel: +81-11-706-7387, Fax: +81-11-706-7820

E-mail: **k-muramatsu@med.hokudai.ac.jp**

Co-corresponding author:

Hideyuki Ujiie, M.D., Ph.D.

Department of Dermatology, Faculty of Medicine and Graduate School of Medicine, Hokkaido University, North 15 West 7, Kita-ku, Sapporo 060-8638, Japan

Tel: +81-11-706-7387, Fax: +81-11-706-7820

E-mail: **h-ujiie@med.hokudai.ac.jp**

Abstract

Aging is a major risk factor for bullous pemphigoid (BP), but aging-induced cutaneous self-tolerance failure remains largely unclear. We examined skin and sera from mice across an age range using direct immunofluorescence (DIF), indirect immunofluorescence (IIF), immunoblotting against recombinant proteins of the dermal–epidermal junction (DEJ), and super-resolution microscopy. Although aged mice developed no blisters or inflammation, they displayed age-dependent linear IgM deposits at the DEJ. Circulating IgM targeted both epidermal and dermal DEJ components and comprised two specificities: age-acquired anti–type XVII collagen (COL17, autoantigen in BP) IgM and lifelong anti–type VII collagen (COL7, autoantigen in epidermolysis bullosa acquisita) IgM. Anti-COL7 IgM persisted across diverse immunopathological models and was reduced in B-1a–deficient mice, supporting a natural antibody origin. We propose a model in which lifelong anti-COL7 natural IgM coexists with aging-driven emergence of anti-COL17 IgM, suggesting a subclinical pre-BP state.

Introduction

The interaction between the immune system and self-antigens is a dynamic process that changes throughout an individual's lifespan. From early in life, the body produces a repertoire of natural antibodies, predominantly of the IgM isotype, which are largely generated by B-1a cells without prior exposure to external antigens[1]. These antibodies serve as a critical first line of defense against invading microbes such as bacteria and viruses. They form a key component of innate immunity and can recognize a variety of self-structures as part of normal physiological homeostasis[1–5].

In contrast, advancing age is accompanied by immunosenescence, a progressive dysregulation of the immune system that can disrupt central and peripheral self-tolerance and increase susceptibility to autoimmune diseases[6,7]. This age-associated immune dysfunction is a major risk factor for various autoimmune conditions, including rheumatoid arthritis (RA), systemic lupus erythematosus (SLE), and autoimmune bullous disease, as evidenced by their more common diagnosis in adulthood[8–10]. Bullous pemphigoid (BP) is the most common autoimmune bullous disease, which predominantly affects the elderly[11–15]. BP is characterized by the formation of tense bullae primarily on the skin and mucous membranes, caused by IgG autoantibodies against type XVII collagen (COL17) and BP230[16–20].

Although the exact pathogenesis of BP is not fully understood, intrinsic and environmental factors have been implicated in its development. Besides aging, which is the most significant predisposing factor[10,11,13], various triggers have been reported, including radiation, ultraviolet exposure, burns, trauma, infection, vaccines, and the use of certain medications such as programmed cell death 1 (PD-1) inhibitors and dipeptidyl peptidase-4 (DPP-4) inhibitors[14,21–28]. Furthermore, dysfunction of regulatory T (Treg) cells, which are crucial for peripheral immune tolerance, has been suggested to contribute to BP pathogenesis[29,30]. In addition, the successful results of an open-label study of BP treated with interleukin 2 therapy were reported, which support BP involvement in the disruption of peripheral immune tolerance by Treg[31]. Recently, it was reported that aging causes immunoglobulin deposition in various organs, contributing to systemic aging[32]. However, the precise mechanisms linking aging and the breakdown of immunotolerance in the skin remain largely unknown.

To elucidate the early events in this age-associated loss of cutaneous immune tolerance, we investigated the presence of autoantibodies in the skin and sera of mice across a wide age range. Here, we show that while aged mice do not develop spontaneous skin lesions, they exhibit a progressive, age-dependent deposition of IgM autoantibodies at the dermal-epidermal junction (DEJ). Our investigation revealed two distinct types of

IgM autoantibodies: one targeting COL17, which emerged specifically with age, and the other targeting type VII collagen (COL7), which was present throughout life. This study highlights the distinct origin and age-associated dynamics of these two autoantibodies and suggests that aging reshapes cutaneous humoral autoreactivity before the development of overt autoimmune skin disease.

Results

Aged mice develop subclinical IgM autoantibody deposits at the DEJ

To determine whether aging is associated with spontaneous histopathologic or immunopathologic changes in skin, we first examined the skin of young (0–9 weeks), adult (28–69 weeks) and aged mice (70 weeks or older). Bullae were absent in either group (Fig. 1A). Histopathologic examination revealed few inflammatory cells in the epidermis and dermis, and no subepidermal or intraepidermal blistering in these groups (Fig. 1B). To evaluate the presence of autoantibodies in aged mice, we performed direct immunofluorescence (DIF) on the skin of mice at various weeks of age. DIF showed few DEJ deposits of IgG (Fig. 1C) and C3 (Fig. 1D), whereas DEJ deposition of IgM increased with age (Fig. 1E). No deposition of IgG, IgM or C3 in intercellular spaces (ICS) was detected. To confirm that this reaction was not due to nonspecific reactivity of anti-mouse IgM antibodies, the specimens were stained with four types of anti-mouse IgM antibodies to ensure that there was no difference in staining (Supplementary Fig. 1A-D). Quantification using ImageJ confirmed that DEJ IgM deposition increased with age (Fig. 1F-G, Supplementary Fig. 2A-C). Furthermore, to determine whether known clinical triggers could convert this age-associated IgM deposition into a more pathogenic response, we investigated whether the administration of the inhibitors of dipeptidyl

peptidase 4 (DPP-4 inhibitors) or the inhibitors of programed cell death protein 1 (PD-1) inhibitors, frequently associated with BP in humans[14,26,27,33,34], could induce class switch to IgG in aged mice. Nine mice were assigned to the anti-PD-1 treatment group and five to the isotype control group, and both groups were treated for four months. However, class switching to IgG was not observed in either group, and the extent of IgM antibody deposition remained unchanged (Supplementary Fig. 3). These findings suggest that a subclinical, age-dependent IgM autoantibody to the DEJ does not class-switch to a pathogenic IgG even in the presence of clinical triggers.

Circulating IgM autoantibodies in aged mice target DEJ components

To identify the target antigens of the circulating IgM autoantibodies, we performed indirect immunofluorescence (IIF) using sera from young and aged mice. IIF on normal neonatal murine skin showed linear deposition of IgM in the DEJ (positive/total, 6-week: 1/5, 40-week: 4/5, 99-week: 4/5; Fig. 2A-B). These findings indicate that aged mice produce circulating IgM autoantibodies that target DEJ proteins.

Identification of age-acquired anti-COL17 IgM antibodies and lifelong anti-COL7 IgM antibodies

Among the proteins that constitute the hemidesmosome, COL17, BP230, and several others are recognized as major targets of autoantibodies[16,35]. Among these proteins, COL17 and BP230, along with COL7, are well-known autoantigens in autoimmune blistering diseases. To investigate the reactivity of mouse sera to the major DEJ antigens, we prepared recombinant proteins of murine COL17, BP230, Laminin α3, Laminin β3, Laminin γ1, and Laminin γ2 as major hemidesmosomal proteins, and COL7 as a structural component of anchoring fibrils (Supplementary Fig. 4), and performed immunoblotting using each recombinant DEJ protein as the substrate. In addition to unpurified sera, sera were purified to characterize these IgM antibodies further. For this purpose, we used protein L beads, which selectively bind immunoglobulins containing the VκI light chain. This allowed us to assess the contribution of IgM antibodies containing the VκI light chain. Using unpurified sera, 1 of 10 samples from 4-week-old mice (young) and 16 of 30 samples from 70 to 76-week-old mice (aged) reacted with COL17 (Fig. 3A). We next purified sera with protein L beads, which bind VκI-bearing mouse immunoglobulins, thereby enriching VκI-containing mouse IgM while effectively removing serum impurities. 0 of 5 sera from 4-week-old mice, 2 of 5 sera from 33-week-old mice, 0 of 5 sera from 57-week-old mice and 0 of 5 sera from 116-week-old mice reacted with COL17 (Fig. 3B). These results suggest that aging is associated with the emergence of anti-

COL17 IgM lacking the VκI light chain.

We performed the same approach using COL7 as the antigen. Using unpurified sera, 9 of 10 samples from 6-week-old mice (young) and 10 of 10 sera from 77-week-old mice (aged) reacted with COL7 (Fig. 3C). Across additional age group, using serum purified with Protein L beads, 3 of 5 sera from 4-week-old mice, 4 of 5 sera from 33-week-old mice, 3 of 5 sera from 57-week-old mice and 5 of 5 sera from 116-week-old mice reacted with COL7 (Fig. 3D). Sera from young and aged mice did not react with Laminin α3, Laminin β3, Laminin γ1, Laminin γ2 and BP230 tested (Supplementary Fig. 5). Together, these findings indicate a dichotomous pattern of age-associated autoimmunity, characterized by the emergence of age-acquired anti-COL17 IgM, in contrast to a lifelong, VκI-restricted anti-COL7 IgM consistent with the properties of a natural antibody, predominantly IgM antibodies produced in the absence of deliberate immunization and characterized by low-affinity, broad reactivity to self- and microbial antigens.

IgM deposited at the DEJ colocalizes with both COL17 and COL7

Having identified circulating anti-COL17 and anti-COL7 IgM in aged mice, we next sought to determine whether these antibody specificities correspond to the IgM deposits observed at the DEJ. To address this, we used super-resolution microscopy to examine

the *in situ* colocalization of IgM with COL17 and COL7. Skin sections were co-stained with IgM together with either anti-COL7 antibodies or anti-COL17 antibodies, and colocalization was assessed across four different age groups (4-week, 28-week, 52-week and 111-week). We found that in 4-week-old mice, IgM deposition at the DEJ was barely detectable, precluding reliable assessment of colocalization. However, in mice aged 28 weeks and older, IgM signals overlapped with both anti-COL7 and anti-COL17 staining (Fig. 4A-B). These findings indicated that IgM deposits at the DEJ are in extremely close proximity to both COL7 and COL17.

Anti-COL7 IgM production is maintained across diverse immunopathological states

Our initial finding that circulating anti-COL7 antibody is present even in young, healthy mice suggested it may represent a constitutive component of the natural antibody repertoire rather than a product of age-associated immunosenescence. To test the robustness and generality of this presence, we examined whether anti-COL7 IgM production is maintained across several models of severe immunodeficiency and immune dysregulation.

We first addressed central tolerance. Bulk RNA sequencing of medullary thymic epithelial cells (mTECs) revealed no significant differences in the expression of DEJ

genes between aged and young mice (Fig. 5A). We then examined *Aire*-knockout (Aire-KO) mice, a model of impaired central tolerance, as the *Aire* gene is essential for maintaining central immune tolerance[36]. As expected in an autoimmune-prone model, sera from *Aire*-KO mice contained anti-COL7 IgM (4 of 5 positive) (Fig. 5B).

Next, we assessed peripheral tolerance using scurfy mice, which lack functional Treg cells. Like wild-type mice, anti-COL7 IgM was readily detected in scurfy mice sera (4 of 5 positive) (Fig. 5C).

Finally, given that BP is associated with type 2 inflammation [37], we examined *Stat6*-KO mice, which are reduced in type 2 immune response. Even in this profoundly altered cytokine environment, anti-COL7 IgM production was maintained in all 5 mice tested (5/5 positive) (Fig. 5D). Together, these findings indicate that anti-COL7 IgM represents an intrinsic component of the murine antibody repertoire, rather than arising as a consequence of defects in central or peripheral tolerance, or dysregulation of type 2 immune response.

Mice lacking B-1a cells show a substantial loss of anti-COL7 IgM antibodies

Natural antibodies are thought to originate largely from B1a cells [3,38]. Given our earlier findings suggesting that anti-COL7 IgM antibodies may be natural antibodies, we aimed

to test whether this autoreactivity is diminished in B1a cell-deficient mice. For this purpose, we used CBA/N mice, a well-established model lacking B1a cells and natural antibodies due to a Btk defect [39,40] (Fig. 6A-B). We purified IgM from the sera of CBA/N mice and assessed anti-COL7 reactivity in the purified IgM by WB. The results showed that CBA/N mice lacked most anti-COL7 IgM reactivity (Fig. 6C).

While our primary experiments were conducted using C57BL/6J mice, we additionally examined other strains to confirm that this phenomenon is not specific to the C57BL/6J strain. We analyzed sera from SJL mice, which are prone to autoantibody production, and BALB/c mice, which are widely used in immunologic studies. WB showed anti-COL7 IgM in 3 of 5 SJL mice and 3 of 5 BALB/c mice (Supplementary Fig. 6), indicating that anti-COL7 IgM is intrinsically produced regardless of strains. Collectively, the marked reduction of anti-COL7 IgM in B-1a–deficient CBA/N mice, together with its preservation in other strains, supports the conclusion that anti-COL7 IgM constitutes a natural antibody predominantly produced by the B-1a lineage.

Discussion

This study reveals two distinct and previously uncharacterized patterns in the age-associated evolution of cutaneous autoreactivity. Our primary finding is that aging in mice is associated with the de novo emergence of IgM autoantibodies against COL17, a key autoantigen in BP. Notably, this occurs in the absence of overt skin lesions, consistent with a subclinical autoimmune state. In contrast, our second major finding is the persistent, lifelong presence of IgM autoantibodies targeting COL7, which we interpret as a natural antibody response predominantly attributable to the B-1a lineage. Collectively, these findings distinguish age-acquired autoreactivity from the lifelong natural antibody repertoire and provide a conceptual framework for understanding early events underlying age-associated erosion of cutaneous immune tolerance.

Our first observation is that aging is associated with the emergence of IgM antibodies against COL17 in mice. Epidemiologic studies have linked advancing age with autoimmune diseases in humans, including rheumatoid arthritis, systemic lupus erythematosus, and BP[10,13]. BP incidence increases with age, with a marked rise after 70 years[10,16,17]. BP is a DEJ-targeting autoimmune blistering disease, whereas pemphigus vulgaris (PV) and pemphigus foliaceus (PF) are intraepidermal blistering diseases driven by autoantibodies against keratinocyte cell–cell adhesion molecules. In contrast, PV and

PF are more commonly present in individuals in their 40s to 50s[41]. In our study, IgM deposition at the dermal–epidermal junction (DEJ) was absent at 4 weeks but became detectable by 30 weeks, an age roughly corresponding to the late 30s in humans.[42] By contrast, IgG and C3 deposition at the DEJ was minimal. Given the established role of complement in BP pathogenesis[43,44], the predominance of IgM deposition without detectable C3 at the DEJ represents a deviation from the canonical pathogenic model. Furthermore, neither IgM, IgG, nor C3 was deposited in ICS throughout the observation period. Although BP and pemphigus vulgaris are both autoimmune blistering diseases, their differing ages of onset in humans may reflect divergent mechanisms within this disease spectrum[12]. IgM pemphigoid, defined by linear IgM deposition at the DEJ, has been reported to present with BP-like features[45,46]. However, no rash developed in our mice. Collectively, these findings indicate that age-associated anti-COL17 IgM reflects a subclinical autoimmune state and is insufficient on its own to cause BP-like disease in mice.

The second finding was that IgM antibodies to COL7, the major autoantigen in epidermolysis bullosa acquisita (EBA), were present in mice regardless of their age. IgG antibodies to COL7 were also detected in scurfy mice lacking regulatory T cells (Treg)[30]. This strongly suggests that those systems are not involved in the production of COL7-

IgM antibodies. To investigate the association between COL7-IgM and central immune tolerance, we evaluated mRNA gene expression of mTEC by bulk RNA-sequenceing and found no increases or decreases in genes such as *Col17a1* and *Col7a1* for DEJ component proteins between young and aged mice. Furthermore, we found that *Aire*-KO mice also develop autoantibodies against COL7, suggesting that these autoantibodies are poorly related to central immune tolerance.

The cellular origin of anti-COL7 IgM is consistent with the natural antibody compartment. Natural IgM is a core feature of innate-like humoral immunity and is conserved across mouse strains. B-1 cells arise early in ontogeny and characteristically produce IgM with relatively restricted variable gene usage, enabling broad reactivity in the absence of prior antigen exposure[3,47,48]. In mice, the immunoglobulin light-chain repertoire is highly diverse at the κ locus (with >100 Vκ segments) but comparatively limited at the λ locus (3 Vλ segments)[49]. To probe whether anti-COL7 IgM exhibits repertoire restriction, we used protein L–based purification, which enriches immunoglobulins bearing VκI light chains. Notably, anti-COL7 reactivity was retained after protein L purification, whereas anti-COL17 reactivity was diminished, consistent with broader light-chain usage among age-acquired anti-COL17 IgM and more restricted usage among anti-COL7 IgM[50–52]. The detection of anti-COL7 IgM across multiple

strains, including C57BL/6J, SJL, and BALB/c, further supports that this response is conserved in mice. Natural antibodies contribute to host defense against bacteria and other organisms[53,54], raising the possibility that anti-COL7 IgM may confer an advantage in early-life environmental exposures. Although the biological significance of anti-COL7 IgM remains unclear, its origin within the natural antibody repertoire suggests a potential role in fitness against microbe-rich habitats, such as soil-associated environments; further studies will be required to define its physiological function. Collectively, these findings support the interpretation that anti-COL7 IgM represents a repertoire-restricted natural autoantibody.

Although the prevalence of BP is higher than EBA in humans[55,56], EBA mouse models are generally easier to establish than BP mouse models[57–59]. One potential explanation is the presence of baseline autoreactivity to COL7 in mice, which may facilitate immune response following COL7 immunization protocols.

In addition to immunoblotting, super-resolution microscopy indicated close spatial proximity between IgM deposits at the DEJ and COL17 or COL7. The spatial resolution of a typical confocal microscope is 200 nm, while that of a typical super-resolution microscope is 100 nm[60]. The IgM and COL17 or COL7 antibodies were therefore shown to be at lesser distances.

Since there have been a number of reports of BP associated with PD-1 and DPP-4 inhibitors[14,24–27], we calculated and administered the human dose based on body weight for the PD-1 and DPP-4 inhibitor administration experiments. However, neither erythema nor bullae developed, and the linear IgM deposition at the DEJ did not undergo class switching to IgG. One possible reason is that the homology of COL17 between mice and humans is approximately 86%[61]. Another explanation for the absence of rash is that DPP-4 (CD26) functions differently in mice than in humans, as reported previously[62]. While PD-1 blockade has been linked to specific T-cell responses implicated in BP[63], it is unknown whether such pathogenic T-cell populations were induced or present in these mice, which may also explain why neither class switching nor clinical disease developed.

A limitation of this study is that our analyses were confined to mice. Notably, the presence of circulating anti-COL7 IgM in young mice did not translate into readily detectable IgM deposition at the DEJ, suggesting that circulating autoreactivity and tissue deposition are separable phenomena. Because circulating IgM reactivity can be markedly reduced by freeze–thaw cycles, we performed these assays using fresh, non-frozen sera; nevertheless, we still observed a dissociation between antigen reactivity in circulation and in situ IgM deposition. This finding further supports the notion that circulating autoreactivity and tissue deposition represent distinct processes. Age-associated changes

in antigen accessibility, vascular permeability, or local clearance mechanisms may lower the threshold for IgM retention at the DEJ.

In conclusion, this study delineates the dynamic relationship between the immune system and cutaneous self-antigens across the lifespan. We propose a model in which lifelong anti-COL7 natural antibodies may contribute to immune homeostasis from early life, while the process of aging induces a breakdown of tolerance to COL17. Our findings may provide a foundation for defining and clarifying the early preclinical steps by which aging increases susceptibility to autoimmune diseases and for clarifying the physiological roles of the natural antibody repertoire.

Methods and materials

Animals

C57BL/6J (B6J) female wild-type mice were purchased from Sankyo Labo (Tokyo, Japan). SJL female mice and BALB/c mice were purchased from Sankyo Labo (Tokyo, Japan). Female heterozygous C57BL/6J.Cg-Foxp3sf/J mice were purchased from the Jackson Laboratory (Bar Harbor, ME) and bred to C57BL/6J wild-type male mice (CLEA Japan, Tokyo, Japan) to generate hemizygous male offspring (scurfy mice). *Stat6*$^{-/-}$ mice were purchased from the Jackson Laboratory (Bar Harbor, ME). AIRE-deficient (*Aire* KO) mice were obtained from Jackson Laboratory (Bar Harbor, ME).

Mice were classified into three age groups: young (0–9 weeks), adult (28–69 weeks), and aged (70 weeks or older). Mice between 10 and 27 weeks of age were not included in this study.

All animal procedures were performed according to guidelines provided by the Hokkaido University Institutional Animal Care and Use Committee under an approved protocol (approval number: #19-0029).

Direct immunofluorescence studies

A direct immunofluorescence (DIF) study was performed on the tail skin samples from

mice. Mouse skins were mounted and snap frozen into optimal cutting temperature compound, and 5 μm cryosections were prepared. The sections were blocked with 0.5% fish gelatin at room temperature for 1 h and incubated with Abs, including Alexa Fluor 488 AffiniPure Goat Anti-Mouse IgM, μ chain specific (Jackson Immunoresearch, 115-545-020, 1:1000), Alexa Fluor 488 AffiniPure Rabbit Anti-Mouse IgG, Fcγ fragment specific (Jackson Immunoresearch, 315-545-008, 1:1000) and murine C3 (mC3; MP Biomedicals, Solon, OH, 1:100) at room temperature for 1 h. Alexa Fluor 488 $F(ab)_2$ Goat anti-mouse IgM (Jackson Immunoresearch, 115-546-075, 1:1000), Alexa Fluor 488 AffiniPure Goat Anti-Mouse IgM, μ chain specific (Invitrogen, A21042) and Alexa Fluor 488 AffiniPure Rabbit Anti-Mouse IgM, μ chain specific (Jackson Immunoresearch, 315-545-020, 1:1000) were also used as IgM antibodies.

For Fig. 1F and Fig. 1G, all samples were processed in parallel in a single staining run under identical antibody incubation conditions and imaged using identical acquisition settings, including exposure time, illumination intensity, and detector gain.

Indirect immunofluorescence studies

Indirect immunofluorescence (IIF) study was performed with the tail skin samples from the neonatal mice as the antigen. All mouse sera were concentrated with Pierce Protein L

Magnetic Beads (Thermo Scientific, 88849). The sections were blocked with 0.5% fish gelatin at room temperature for 1 h and incubated with 6-week, 40-week and 90-week mice sera, diluted with Can Get Signal immunostain Immunoreaction Enhancer Solution (TOYOBO, Tokyo, Japan NKB-601) at 4 ℃ overnight and detected by secondary Abs, Alexa Fluor 488 F(ab)2 Goat anti-mouse IgM (Jackson Immunoresearch, 115-546-075, 1:1000).

Images were captured with fluorescence microscopy (Olympus, BX51, Tokyo, Japan).

To minimize potential loss of IgM reactivity, freshly collected sera were immediately subjected to affinity purification using Protein L beads. The resulting Protein L–purified immunoglobulin fractions were used as primary antibodies for IIF on the same day. Neither the sera nor the purified immunoglobulin fractions were frozen before IIF analysis. For Fig. 2A, all samples were processed in parallel in a single staining run under identical antibody incubation conditions and imaged using identical acquisition settings, including exposure time, illumination intensity, and detector gain.

ImageJ analysis

The DIF images were visually inspected, and a red line was manually drawn along the

DEJ. Rectangular regions, 10 μm in width and centered on the red line, were used to quantify the Alexa Fluor fluorescence intensity. Specifically, within each rectangle, the maximum fluorescence intensity along each line perpendicular to the red line was determined, and the resulting maximum values were then averaged along the red line. The analysis was performed using a custom-written plugin for ImageJ (National Institutes of Health, USA)[64].

Double staining

Double staining study was performed on the tail skin samples from 4-week, 28-week, 52-week and 111-week mice tails. Two types of double staining were performed using anti-COL17 antibody (abcam, ab184996) or anti-COL7 antibody (generated by our group, as previously described[65]) as primary antibody, and Goat anti-Rabbit IgG (H+L) Secondary antibody, Alexa Fluor® 647 (Thermo, A-21244, 1:1000) and Alexa Fluor® 488 AffiniPure Goat Anti-Mouse IgM, μ chain specific (Jackson Immunoresearch, 115-545-020, 1:1000) as secondly. Images were acquired with DeepSIM (CrestOptics, Italy).

Recombinant proteins

Recombinant full-length murine COL17 protein with a FLAG-tag at the N-terminus was

generated by our department, as previously described[17,66]. Three fragments of recombinant murine BP230 with His-tag at the C-terminus were generated as previously described[29]. Other DEJ proteins were purchased as follows. Each recombinant full-length murine protein, *Lamc1* (MR227404; OriGene, Rockville, MD), *Lamb3* (MR211741; OriGene, Rockville, MD), *Lamc2* (MR222717; OriGene, Rockville, MD) and *Col7a1* (MR215786; OriGene, Rockville, MD) was transiently expressed in HEK293 cells or Lenti-X 293T cells transfected with Lipofectamine 3000 (Thermo Fisher Scientific, MA, L3000015). Two fragments of the murine *Lama3* (accession number NM_010680.1), middle (1,002 base pairs, aa1656-1985) and C-terminal (1,740 base pairs, aa2756-3330) portions, were generated as previously reported[67]. Middle and C-terminal murine *Lama3* were cloned into the expression vector pCMV-3Tag-3A and pcDNA3.1(+)-C-DYK vector, respectively. Middle and C-terminal murine *Lama3* were transiently expressed in HEK293 cells transfected with Lipofectamine 3000 (Thermo Fisher Scientific, MA, L3000015). Only murine BP230 proteins were purified with AMICON Ultra 15 mL (MERCK, UFC910024) and Capturem His-Tagged Purification Miniprep Kit (TAKARA, 635710). The other DEJ proteins were purified with anti-DDDDK-tag mAb-magnetic beads (M185-11R, MBL, Japan) and FLAG peptide (F3290, Millipore, MA). Each recombinant murine protein was confirmed for protein expression with the following

antibodies: anti-COL7 antibody (previously described[65]), anti-Laminin β3 antibody (abcam, ab150385), anti-Laminin γ1 antibody (Santa Cruz, sc-17751), and anti-Laminin γ2 antibody (Santa Cruz, sc-28330), Anti-DDDDK-tag mAb-HRP-DirecT (MBL, M185-**-7**) or anti-His-tag mAb-HRP-DirecT (MBL, D291-7).

Western blotting with murine recombinant protein fragments

All the above recombinant murine proteins were used as substrates. All protein samples were denatured for 5 minutes at 95℃ with sample buffer (0.25 M Tris-HCl; 8% SDS; 30% glycerol; 0.02% bromophenol blue; 0.3 M β-mercaptoethanol; pH 6.8). Samples were run on a 7% SDS-PAGE system, and electrophoretically transferred onto nitrocellulose membranes (BioRad, CA). After the transfer, the membranes were blocked with 2% skim milk in TBS-Tween for 1 h at RT.

Various week-old mouse sera were used as primary antibody at 4℃ for 16 h. Mouse sera were concentrated with Pierce Protein L Magnetic Beads (Thermo Scientific, 88849). Peroxidase-conjugated AffiniPure Rabbit Anti-Mouse IgM, μ-Chain Specific (JacksonImmunoResearch, 315-035-020, 1:1000) was used as secondary Abs for 1 h at RT. Monoclonal anti-FLAG® M2 antibody-peroxidase-conjugated (Sigma-Aldrich, A8592, 1:1000) was used as a positive control. All antibodies were diluted with 2% skim

milk blocking buffer for 1 h at RT. Signals were visualized with Clarity Western ECL Substrate (BioRad, CA) and captured by the LAS-4000 miniImager (Fujifilm, Lexington, MA) and WSE-6100H Luminograph (ATTO, Japan).

To minimize potential loss of IgM reactivity, freshly collected sera were immediately subjected to affinity purification using Protein L beads. The resulting Protein L–purified serum immunoglobulins were used as primary antibodies for western blotting on the same day. The purified immunoglobulin fractions were not frozen at any point between collection and western blot analysis. For each western blot figure, all samples shown were analyzed in a single experimental run on the same membrane under identical antibody incubation and detection conditions.

Statistical analysis.

All statistical analyses were performed with GraphPad Prism 9.2.0 (GraphPad Software, San Diego, CA), evaluating by unpaired t-test (Fig. 1F) and Dunnett's multiple comparisons test (Fig. 1G).

Isolation and preparation of medullary thymic epithelial cells (mTECs)

Thymi were harvested from mice and subsequently digested into a single-cell suspension

using DNase I (Roche, 11-284-932-001) and Liberase™ Thermolysin Medium (Roche, 05-401-119-001). To enrich for mTECs, thymocytes were depleted from the cell suspension using Dynabeads™ Mouse Pan T (Invitrogen, 11443D) and a DynaMag™ Spin magnet according to the manufacturer's instructions.

Flow cytometry staining and sorting of mTECs

The resulting cell suspension was stained with the following antibodies for flow cytometry analysis and sorting: PerCpCy5.5-conjugated anti-mouse CD45 monoclonal antibody (BioLegend, 103131), APC-Fire750-conjugated anti-mouse IA/IE mAb (BioLegend, 107651), PE-Cy7-conjugated anti-mouse EpCAM mAb (BioLegend, 118316), PE-conjugated anti-mouse Ly51 mAb (BioLegend, 108307), APC-StreptAvidin-conjugated anti-mouse UEA-1 mAb (eBioscience, 17-4317-82). mTECs were sorted using a FACSAria III cell sorter (BD Biosciences).

RNA Isolation of mTECs

Total RNA was isolated from the sorted mTECs using TRIzol™ Reagent (Invitrogen, 15596026) following the manufacturer's protocol.

Bulk RNA-sequencing and analysis

Each mRNA of the mTEC cells was extracted from the cultured cells with the Qiagen RNeasy Mini kit (Qiagen). The extracted mRNA had sufficient quality for RNA-seq, with RIN values of 8 or higher as a result of analysis using the 2100 Bioanalyzer system (Agilent). Purified total RNA (3 ng) was used for RNA library preparation, according to the instructions of the NEBNext Ultra II Directional RNA Library Prep Kit for Illumina (NEB). The RNA libraries were sequenced on an Illumina NextSeq 500 system with 75-nt-long reads. Gene expression levels between aged mice and young mice were compared. Differentially expressed genes were identified based on a $\geq$ 2-fold change and $p \leq 0.05$ after DESeq correction. All data analyses were conducted using Strand NGS ver4.0 (Strand Life Sciences Pvt. Ltd.).

Flow cytometry staining of B1 cells

The resulting cell suspension was stained with the following antibodies for flow cytometry analysis: LIVE/DEAD™ Fixable Near-IR Dead Cell Stain Kit, for 633 or 635 nm excitation (Invitrogen™, L10119), BB515 Rat Anti-Mouse CD19 (BD Horizon™, 564509), PE/Cyanine7 anti-mouse/human CD45R/B220 (BioLegend, 103222), Brilliant Violet 510™ anti-mouse CD5 (BioLegend, 100627), PerCP/Cyanine5.5 anti-mouse

CD43 (BioLegend, 143219), APC anti-mouse IgD (BioLegend, 405713), PE anti-mouse IgM (BioLegend, 406507). B1a cells were detected by flow cytometric analysis using a FACSCanto II system (BD Pharmingen).

Vildagliptin administration

Aged mice administered vildagliptin (Sigma, CDS022675) in their drinking water at an estimated dose of 0.24 mg per mouse per day (n = 7). Untreated control mice received regular drinking water (n = 9). Mice were evaluated for up to 4 months.

Anti-PD-1 antibody administration

Aged mice were intraperitoneally administered 200 μg of an InVivoplus anti-mouse PD-1 antibody (CD279) (Bio X Cell, BE0146) twice weekly for 4 months (n = 5). Control mice received 200 μg of an InVivoMAb rat IgG2a isotype control antibody (Bio X Cell, BE0089) according to the same dosing schedule (n = 3).

CONFLICTS OF INTEREST

The authors have declared that no conflict of interest exists.

ACKNOWLEDGEMENTS

We thank Miho Yamashita and Kayo Miyazaki for their technical assistance. We also thank the Global Facility Center at Hokkaido University for allowing us to conduct super-resolution microscope analysis. This work was supported by JSPS KAKENHI JP20K21590 (to H.U.), JSPS KAKENHI JP21H02938 (to H.U.), JSPS KAKENHI JP25K02670 (to H.U.), JSPS KAKENHI JP24K19158 (to K.M.), and by AMED under grant number JP20ek0109430 (to H.U.), JP26ek0109792 (to H.U.) and JP266f0137006 (to K.M.), Project for Junior Scientist Promotion of Hokkaido University (to H.U.), Japanese Dermatological Association Research Grant (Novartis Pharma K.K. Grant) (to H.U.), and The Naito Foundation (to H.U.).

AUTHOR CONTRIBUTIONS

Conceptualization: CS, KM, HU; Investigation: CS, KM, YF, KS, UT; Project Administration: KM, HU; Validation: KM, NY, SK, TK, TI, KI, HU; Formal Analysis: HK, YF, YO; Writing - Original Draft Preparation: CS, KM; Writing – Review and Editing: NY, SK, TK, SM, YM, TI, KI, KN, HI, HY, YF, YO, KS, UT, HU; Supervision: HU.

Chihiro Shiiya[1], Ken Muramatsu[1], Norihiro Yoshimoto[1], Sho Katayama[1], Takuya Kawamura[1], Shoko Mai[1], Yosuke Mai[1], Takamasa Ito[1], Kentaro Izumi[1], Ken Natsuga[1], Hiroaki Iwata[2], Hiroyuki Kitahata[3], Yoichiro Fujioka[4], Yusuke Ohba[4], Kentaro Saito[5], Utano Tomaru[6], Yoshinori Hasegawa[7], Hideyuki Ujiie[1]

Reference

1. Hardy, R. R. & Hayakawa, K. A developmental switch in B lymphopoiesis. *Proc. Natl. Acad. Sci.* **88**, 11550–11554 (1991).

2. Duan, B. & Morel, L. Role of B-1a cells in autoimmunity. *Autoimmun. Rev.* **5**, 403–408 (2006).

3. Baumgarth, N. The double life of a B-1 cell: self-reactivity selects for protective effector functions. *Nat. Rev. Immunol.* **11**, 34–46 (2011).

4. Suchanek, O. & Clatworthy, M. R. Homeostatic role of B-1 cells in tissue immunity. *Front. Immunol.* **14**, 1106294 (2023).

5. Mattos, M. S., Vandendriessche, S., Waisman, A. & Marques, P. E. The immunology of B-1 cells: from development to aging. *Immun. Ageing* **21**, 54 (2024).

6. Shirafkan, F., Hensel, L. & Rattay, K. Immune tolerance and the prevention of autoimmune diseases essentially depend on thymic tissue homeostasis. *Front. Immunol.* **15**, 1339714 (2024).

7. Wang, Y., Dong, C., Han, Y., Gu, Z. & Sun, C. Immunosenescence, aging and successful aging. *Front. Immunol.* **13**, 942796 (2022).

8. Pons-Estel, G. J., Alarcón, G. S., Scofield, L., Reinlib, L. & Cooper, G. S. Understanding the Epidemiology and Progression of Systemic Lupus Erythematosus. *Semin. Arthritis Rheum.* **39**, 257–268 (2010).

9. Serhal, L., Lwin, M. N., Holroyd, C. & Edwards, C. J. Rheumatoid arthritis in the elderly: Characteristics and treatment considerations. *Autoimmun. Rev.* **19**, 102528 (2020).

10. Goronzy, J. J., Li, G., Yang, Z. & Weyand, C. M. The janus head of T cell aging - autoimmunity and immunodeficiency. *Front. Immunol.* **4**, 131 (2013).

11. Jung, M., Kippesb, W., Messer, G., Zillikens, D. & Rzany, B. Increased risk of bullous pemphigoid in male and very old patients: A population-based study on incidence. *J. Am. Acad. Dermatol.* **41**, 266–268 (1999).

12. Marazza, G. *et al.* Incidence of bullous pemphigoid and pemphigus in Switzerland: a 2-year prospective study. *Br. J. Dermatol.* **161**, 861–868 (2009).

13. Kridin, K. & Ludwig, R. J. The Growing Incidence of Bullous Pemphigoid: Overview and Potential Explanations. *Front. Med.* **5**, 220 (2018).

14. Russo, F. *et al.* The possible and intriguing relationship between bullous pemphigoid and melanoma: speculations on significance and clinical relevance. *Front. Immunol.* **15**, 1416473 (2024).

15. Ujiie, I. *et al.* Clinical characteristics and outcomes of dipeptidyl peptidase-4 inhibitor-associated bullous pemphigoid patients: A retrospective study. *J. Am. Acad. Dermatol.* **92**, 561–564 (2025).

16. Schmidt, E. & Zillikens, D. Pemphigoid diseases. *The Lancet* **381**, 320–332 (2013).

17. Nishie, W. Update on the pathogenesis of bullous pemphigoid: An autoantibody-mediated blistering disease targeting collagen XVII. *J. Dermatol. Sci.* **73**, 179–186 (2014).

18. Zillikens, D. *et al.* Tight clustering of extracellular BP180 epitopes recognized by bullous pemphigoid autoantibodies. *J. Invest. Dermatol.* **109**, 573–579 (1997).

19. Stanley, J. R., Tanaka, T., Mueller, S., Klaus-Kovtun, V. & Roop, D. Isolation of complementary DNA for bullous pemphigoid antigen by use of patients' autoantibodies. *J. Clin. Invest.* **82**, 1864–1870 (1988).

20. Giudice, G. J. *et al.* Bullous pemphigoid and herpes gestationis autoantibodies recognize a common non-collagenous site on the BP180 ectodomain. *J. Immunol.* **151**, 5742–5750 (1993).

21. Dănescu, S., Chiorean, R., Macovei, V., Sitaru, C. & Baican, A. Role of physical factors in the pathogenesis of bullous pemphigoid: Case report series and a comprehensive review of the published work. *J. Dermatol.* **43**, 134–140 (2016).

22. Sagi, L. *et al.* Autoimmune bullous diseases the spectrum of infectious agent antibodies and review of the literature. *Autoimmun. Rev.* **10**, 527–535 (2011).

23. Ghanaatpisheh, A. *et al.* New-onset or flare-up of bullous pemphigoid associated with COVID-19 vaccines: a systematic review of case report and case series studies. *Front. Med.* **11**, 1293920 (2024).

24. Arai, M., Shirakawa, J., Konishi, H., Sagawa, N. & Terauchi, Y. Bullous Pemphigoid and Dipeptidyl Peptidase 4 Inhibitors: A Disproportionality Analysis Based on the Japanese Adverse Drug Event Report Database. *Diabetes Care* **41**, e130–e132 (2018).

25. Béné, J. *et al.* Bullous pemphigoid and dipeptidyl peptidase IV inhibitors: a case-noncase study in the French Pharmacovigilance Database. *Br. J. Dermatol.* **175**, 296–301 (2016).

26. Siegel, J. *et al.* Bullous disorders associated with anti-PD-1 and anti-PD-L1 therapy: A retrospective analysis evaluating the clinical and histopathologic features, frequency, and impact on cancer therapy. *J. Am. Acad. Dermatol.* **79**, 1081–1088 (2018).

27. Ujiie, H. What's new in the pathogeneses and triggering factors of bullous pemphigoid. *J. Dermatol.* **50**, 140–149 (2023).

28. Mai, Y. *et al.* Bullous Pemphigoid Triggered by Thermal Burn Under Medication With a Dipeptidyl Peptidase-IV Inhibitor: A Case Report and Review of the Literature. *Front. Immunol.* **9**, 542 (2018).

29. Muramatsu, K. *et al.* Regulatory T-cell dysfunction induces autoantibodies to bullous pemphigoid antigens in mice and human subjects. *J. Allergy Clin. Immunol.* **142**, 1818-1830.e6 (2018).

30. Haeberle, S. *et al.* Regulatory T-cell deficiency leads to pathogenic bullous pemphigoid antigen 230 autoantibody and autoimmune bullous disease. *J. Allergy Clin. Immunol.* **142**,

1831-1842.e7 (2018).

31. Xue, R. *et al.* Efficacy and safety of low-dose interleukin 2 in the treatment of moderate-to-severe bullous pemphigoid: A single center perspective-controlled trial. *J. Am. Acad. Dermatol.* S0190962224027300 (2024) doi:10.1016/j.jaad.2024.08.033.

32. Ma, S. *et al.* Spatial transcriptomic landscape unveils immunoglobin-associated senescence as a hallmark of aging. *Cell* S0092867424012017 (2024) doi:10.1016/j.cell.2024.10.019.

33. García-Díez, I. *et al.* Bullous pemphigoid induced by dipeptidyl peptidase-4 inhibitors. Eight cases with clinical and immunological characterization. *Int. J. Dermatol.* **57**, 810–816 (2018).

34. Oya, K., Fujii, M. & Taguchi, S. Development of pemphigus vulgaris during treatment with dipeptidyl peptidase-4 inhibitors: a case report. *Dermatol. Ther.* **34**, e14982 (2021).

35. Zillikens, D. Acquired skin disease of hemidesmosomes. *J. Dermatol. Sci.* **20**, 134–154 (1999).

36. Chan, A. Y. & Anderson, M. S. Central tolerance to self revealed by the autoimmune regulator. *Ann. N. Y. Acad. Sci.* **1356**, 80–89 (2015).

37. Ruan, Y. *et al.* Single-Cell Profiling Unveils the Inflammatory Heterogeneity within Cutaneous Lesions of Bullous Pemphigoid. *J. Invest. Dermatol.* **144**, 2176-2186.e6

(2024).

38. Lutz, H. U., Binder, C. J. & Kaveri, S. Naturally occurring auto-antibodies in homeostasis and disease. *Trends Immunol.* **30**, 43–51 (2009).

39. Hayakawa, K., Hardy, R. R., Parks, D. R. & Herzenberg, L. A. The 'Ly-1 B' cell subpopulation in normal immunodefective, and autoimmune mice. *J. Exp. Med.* **157**, 202–218 (1983).

40. Rawlings, D. J. *et al.* Mutation of Unique Region of Bruton's Tyrosine Kinase in Immunodeficient XID Mice. *Science* **261**, 358–361 (1993).

41. Committee for Guidelines for the Management of Pemphigus Disease *et al.* Japanese guidelines for the management of pemphigus. *J. Dermatol.* **41**, 471–486 (2014).

42. Dutta, S. & Sengupta, P. Men and mice: Relating their ages. *Life Sci.* **152**, 244–248 (2016).

43. Zeng, F. A. P. & Murrell, D. F. Bullous pemphigoid—What do we know about the most recent therapies? *Front. Med.* **9**, 1057096 (2022).

44. Papara, C. *et al.* The relevance of complement in pemphigoid diseases: A critical appraisal. *Front. Immunol.* **13**, 973702 (2022).

45. Boch, K. *et al.* Immunoglobulin M pemphigoid. *J. Am. Acad. Dermatol.* **85**, 1486–1492 (2021).

46. Hirano, Y. *et al.* Super‐resolution imaging detects BP180 autoantigen in

immunoglobulin M pemphigoid. *J. Dermatol.* **49**, 374–378 (2022).

47. Hardy, R. R. B-1 B Cell Development. *J. Immunol.* **177**, 2749–2754 (2006).

48. Yang, Y. *et al.* Distinct mechanisms define murine B cell lineage immunoglobulin heavy chain (IgH) repertoires. *eLife* **4**, e09083 (2015).

49. Collins, A. M. & Watson, C. T. Immunoglobulin Light Chain Gene Rearrangements, Receptor Editing and the Development of a Self-Tolerant Antibody Repertoire. *Front. Immunol.* **9**, 2249 (2018).

50. Björck, L. Protein L. A novel bacterial cell wall protein with affinity for Ig L chains. *J. Immunol. Baltim. Md 1950* **140**, 1194–1197 (1988).

51. Åkerström, B. & Björck, L. Protein L: An Immunoglobulin Light Chain-binding Bacterial Protein. *J. Biol. Chem.* **264**, 19740–19746 (1989).

52. Cremers, G. A. O., Rosier, B. J. H. M., Riera Brillas, R., Albertazzi, L. & De Greef, T. F. A. Efficient Small-Scale Conjugation of DNA to Primary Antibodies for Multiplexed Cellular Targeting. *Bioconjug. Chem.* **30**, 2384–2392 (2019).

53. Cunningham, A. F. *et al.* B1b cells recognize protective antigens after natural infection and vaccination. *Front. Immunol.* **5**, 535 (2014).

54. Stäger, S. *et al.* Natural antibodies and complement are endogenous adjuvants for vaccine-induced CD8+ T-cell responses. *Nat. Med.* **9**, 1287–1292 (2003).

55. Iwata, H. *et al.* Meta-analysis of the clinical and immunopathological characteristics and treatment outcomes in epidermolysis bullosa acquisita patients. *Orphanet J. Rare Dis.* **13**, 153 (2018).

56. Kridin, K., Kneiber, D., Kowalski, E. H., Valdebran, M. & Amber, K. T. Epidermolysis bullosa acquisita: A comprehensive review. *Autoimmun. Rev.* **18**, 786–795 (2019).

57. Ujiie, H. *et al.* A Novel Active Mouse Model for Bullous Pemphigoid Targeting Humanized Pathogenic Antigen. *J. Immunol.* **184**, 2166–2174 (2010).

58. Ludwig, R. J. *et al.* Generation of Antibodies of Distinct Subclasses and Specificity Is Linked to H2s in an Active Mouse Model of Epidermolysis Bullosa Acquisita. *J. Invest. Dermatol.* **131**, 167–176 (2011).

59. Giusti, D. *et al.* Anti-Type VII Collagen Antibodies Are Identified in a Subpopulation of Bullous Pemphigoid Patients With Relapse. *Front. Immunol.* **9**, 570 (2018).

60. *Https://Crestoptics.Com/Introducing-the-Deepsim-Super-Resolution-System-a-Seamless-Evolution-of-Your-Microscopy/*.

61. Li, K., Tamai, K., Tan, E. M. & Uitto, J. Cloning of type XVII collagen. Complementary and genomic DNA sequences of mouse 180-kilodalton bullous pemphigoid antigen (BPAG2) predict an interrupted collagenous domain, a transmembrane segment, and unusual features in the 5'-end of the gene and the 3'-untranslated region of the mRNA.

J. Biol. Chem. **268**, 8825–8834 (1993).

62. Ohnuma, K. *et al.* A novel role for CD26/dipeptidyl peptidase IV as a therapeutic target. *Front. Biosci. Landmark Ed.* **23**, 1754–1779 (2018).

63. Ernst, N. *et al.* Expression of PD‐1 and Tim‐3 is increased in skin of patients with bullous pemphigoid and pemphigus vulgaris. *J. Eur. Acad. Dermatol. Venereol.* **35**, 486–492 (2021).

64. Schneider, C. A., Rasband, W. S. & Eliceiri, K. W. NIH Image to ImageJ: 25 years of image analysis. *Nat. Methods* **9**, 671–675 (2012).

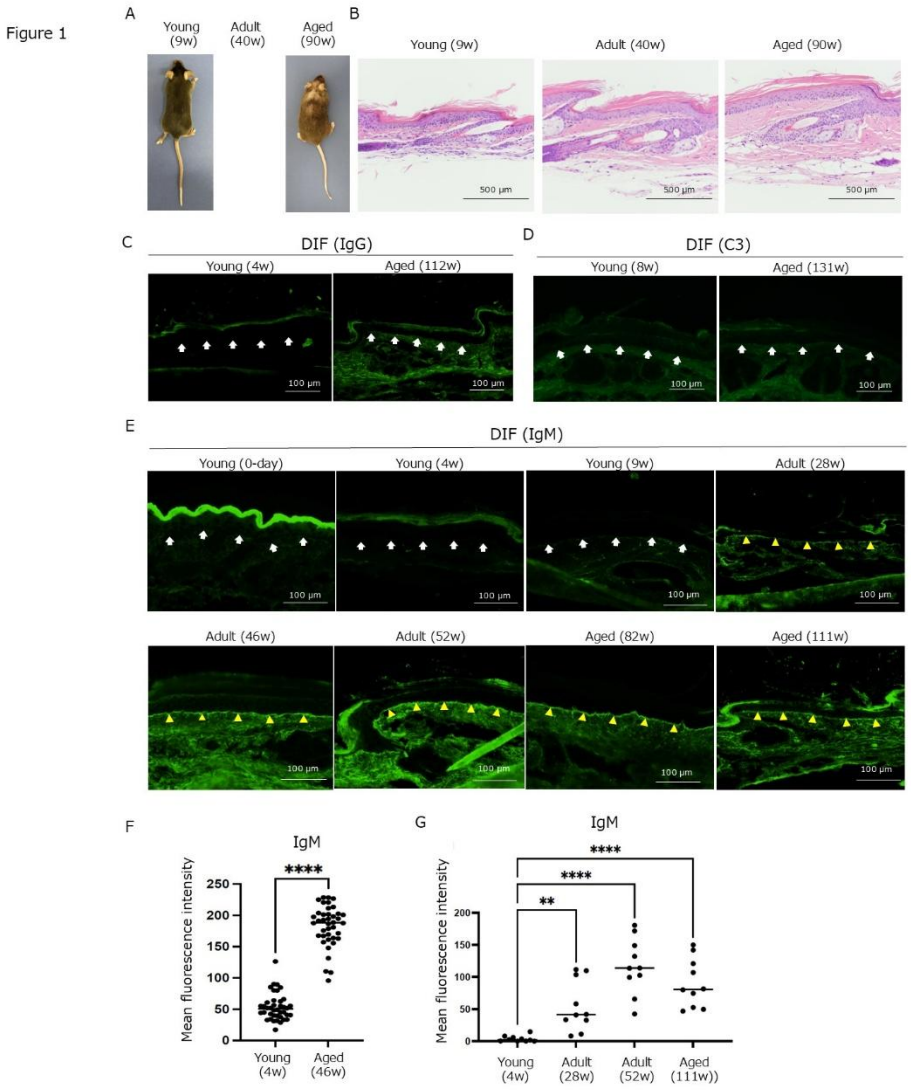
65. Iwata, H. *et al.* B Cells, Dendritic Cells, and Macrophages Are Required To Induce an Autoreactive CD4 Helper T Cell Response in Experimental Epidermolysis Bullosa Acquisita. *J. Immunol.* **191**, 2978–2988 (2013).

66. Toyonaga, E. *et al.* C-Terminal Processing of Collagen XVII Induces Neoepitopes for Linear IgA Dermatosis Autoantibodies. *J. Invest. Dermatol.* **137**, 2552–2559 (2017).

67. Heppe, E. N. *et al.* Experimental Laminin 332 Mucous Membrane Pemphigoid Critically Involves C5aR1 and Reflects Clinical and Immunopathological Characteristics of the Human Disease. *J. Invest. Dermatol.* **137**, 1709–1718 (2017).

Figure legends

Figure 1. The deposition of autoantibodies on mice skin.



(A) Representative gross appearance of young, adult and aged C57BL/6J mice. The aged mouse did not have bullae.

(B) Representative H&E images of young and aged mice. (scale bar 500 μm) (n = 5 per group).

(C) DIF (IgG) of tail skin comparing between 4-week and 112-week. (scale bar 100 μm)

(n = 5 per group). The white arrows indicate the DEJ area without antibody deposition.

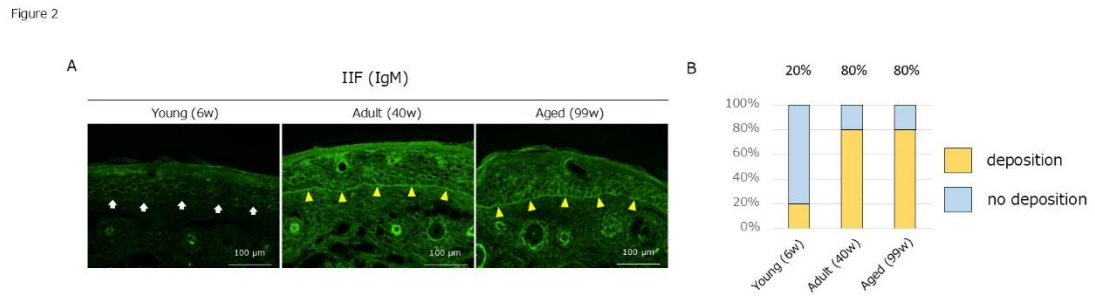
(D) DIF (C3) of tail skin comparing between 8-week and 131-week. (scale bar 100 μm) (n = 5 per group). The white arrows indicate the DEJ area without antibody deposition.

(E) DIF (IgM) of tail skin comparing between 0-day, 4-week, 9-week, 28-week, 46-week, 52-week, 82-week and 111-week. (scale bar 100 μm) (n = 5 per group). The white arrows indicate the DEJ area without antibody deposition. The yellow arrowheads indicate the DEJ area with antibody deposition.

(F) For quantification of IgM deposition, skin specimens were obtained from 20 mice in each age group (4 and 46 weeks). Forty images were acquired from 20 mice per group. ****$p < 0.0001$

(G) The quantification of the IgM antibody deposition was compared between 4-week, 28-week, 52-week and 111-week each 10 specimens. **$p < 0.01$; ****$p < 0.0001$.

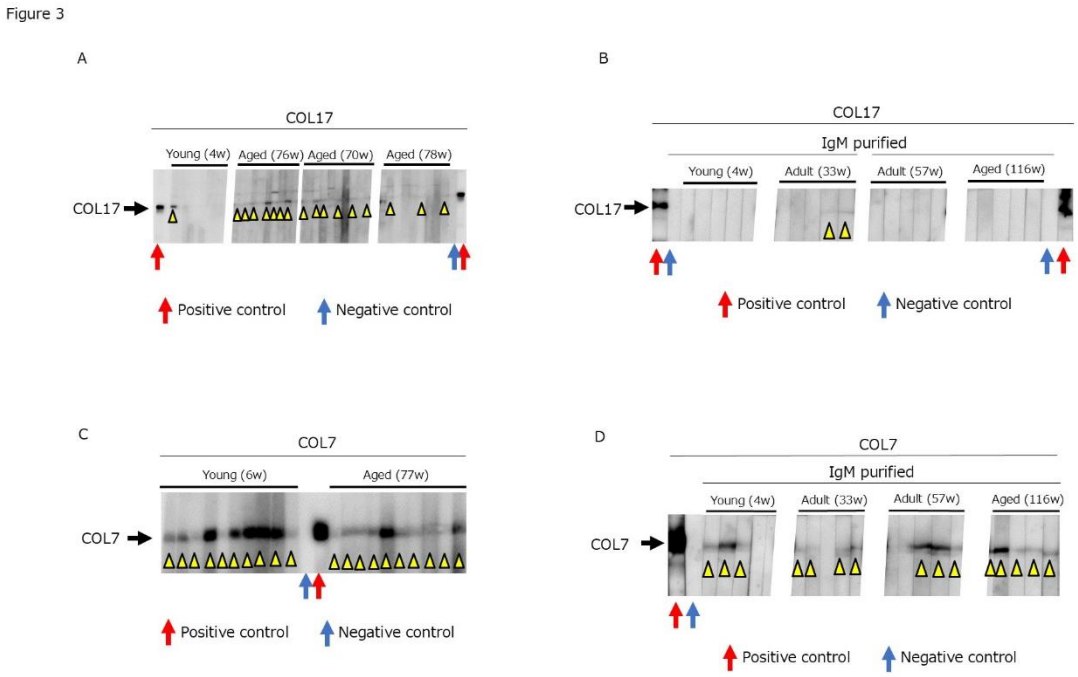
Figure 2. Sera from aged mice react with DEJ proteins.



(A) Indirect immunofluorescence (IIF) analysis on normal neonatal murine skin showed linear deposition of IgM in the DEJ comparing between 6-week, 40-week and 99-week (n = 5 per group). The white arrows indicate the DEJ area without antibody deposition. The yellow arrowheads indicate the DEJ area with antibody deposition.

(B) Positive rates were higher in adult and aged mice.

Figure 3. Evaluation of mouse sera against COL17/COL7 by western blotting



(A) Evaluation of unpurified mouse sera against COL17. Sera from 1/10 4-week-old mice (young mice), 16/30 70 to 78-week-old mice (aged mice) reacted with COL17. The yellow arrowheads indicate the bands corresponding to COL17 recognized by serum IgM antibodies.

(B) Evaluation of purified mouse sera against COL17. Sera from 0/5 4-week-old mice, 2 /5 33 -week-old mice, 0/5 57-week-old mice and 0/5 sera 116-week-old mice reacted with COL17. The yellow arrowheads indicate the bands corresponding to COL17 recognized by serum IgM antibodies.

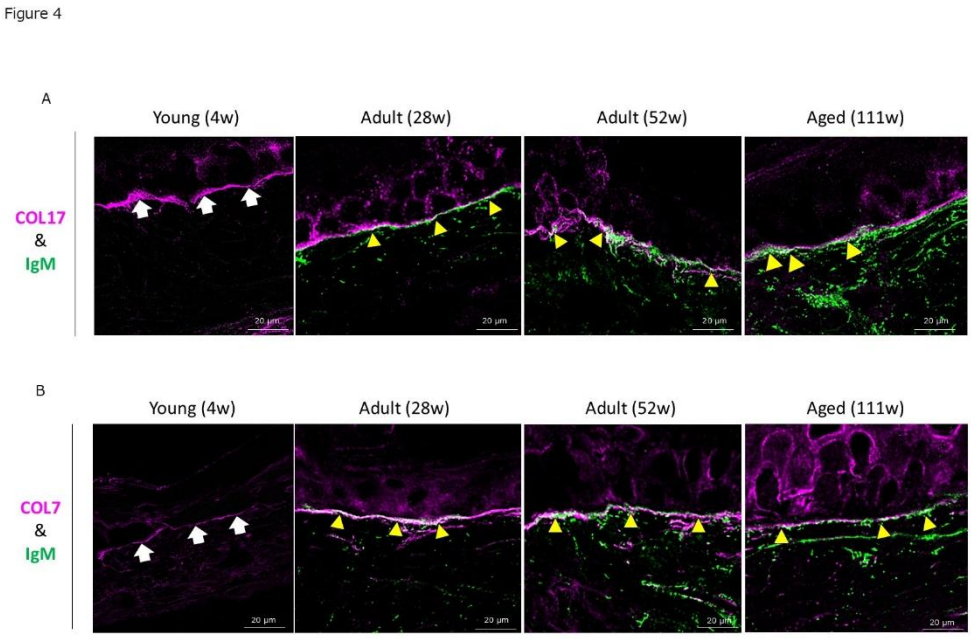
(C) Evaluation of unpurified mouse sera against COL7. Sera from 10 of 10 6-week-old

mice (young mice), 10/10 77-week-old mice (aged mice) reacted with COL7. The yellow arrowheads indicate the bands corresponding to COL17/COL7 recognized by serum IgM antibodies. The yellow arrowheads indicate the bands corresponding to COL7 recognized by serum IgM antibodies.

(D) Evaluation of purified mouse sera against COL7. Sera from 3/5 4-week-old mice, 4/5 33-week-old mice, 3/5 57-week-old mice and 5/5 116-week-old mice reacted with COL7. The yellow arrowheads indicate the bands corresponding to COL7 recognized by serum IgM antibodies.

PC, positive control, detected using Anti-DDDDK-tag mAb-HRP-DirecT; NC, negative control, in which PBS was used instead of the primary antibody, followed by peroxidase-conjugated AffiniPure Rabbit Anti-Mouse IgM (μ-chain specific).

Figure 4. Double staining with anti-IgM antibodies in the skin and anti-COL17 /anti-COL7 antibodies.

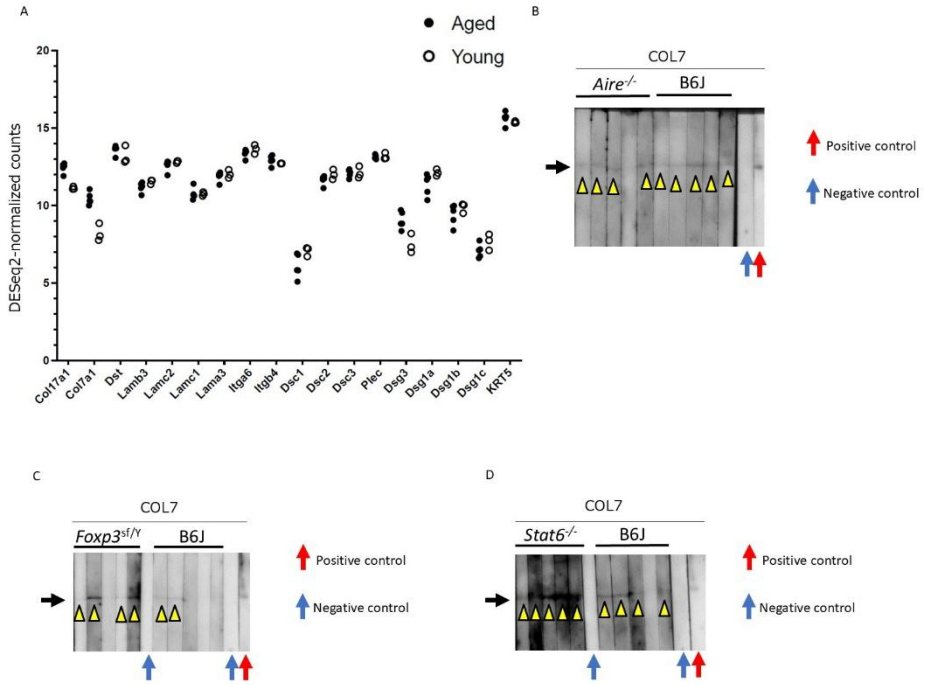


（A）Comparison of deposition between anti-IgM antibodies (Green) and anti-COL17 (Magenta) by age (n = 4 per group). The white arrows indicate the DEJ area without IgM antibody deposition. The yellow arrowheads indicated the location of DEJ.

（B）Comparison of deposition between anti-IgM antibodies (Green) and anti-COL7 (Magenta) by age (n = 4 per group). The white arrows indicate the DEJ area without IgM antibody deposition. The yellow arrowheads indicated the location of DEJ.

Figure 5. Age-independent expression of DEJ protein–encoding mRNAs in mTECs and maintenance of anti-COL7 IgM production across diverse immunopathological states

Figure 5



(A) There were no significant upregulation or downregulation after adjusting for false discovery rate (FDR) between mTECs of aged (81-96 weeks old) and young (6-10 weeks old) mice (p-values ≤ 0.05).

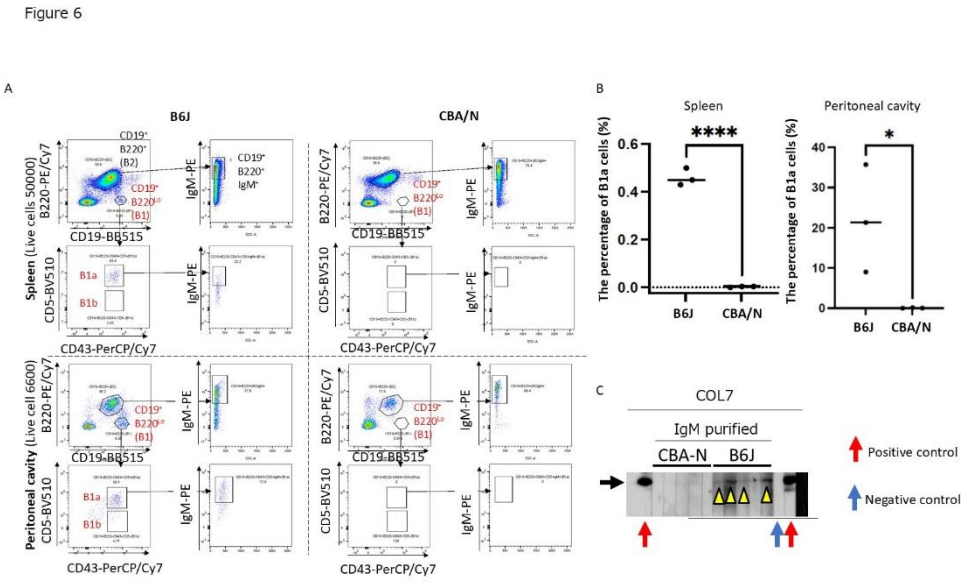
(B) Purified sera from 3/5 4-week-old AIRE-KO mice and 5/5 4-week-old B6J mice against COL7. The yellow arrowheads indicate the bands corresponding to COL7 recognized by serum IgM antibodies.

(C) Purified sera from 4/5 4-week-old scurfy mice and 2/5 4-week-old wild-type mice against COL7. The yellow arrowheads indicate the bands corresponding to COL7 recognized by serum IgM antibodies.

(D) Purified sera from 5/5 4-week-old STAT6-KO mice and 4/5 4-week-old wild-type mice against COL7. The yellow arrowheads indicate the bands corresponding to COL7 recognized by serum IgM antibodies.

PC, positive control, detected using Anti-DDDDK-tag mAb-HRP-DirecT; NC, negative control, in which PBS was used instead of the primary antibody, followed by peroxidase-conjugated AffiniPure Rabbit Anti-Mouse IgM (μ-chain specific).

Figure 6. Reduced detection of serum anti-COL7 antibodies in mice lacking B-1a cells.

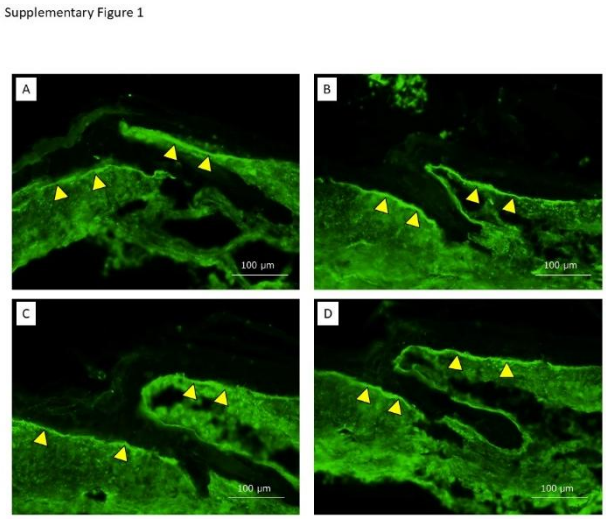


(A) Flow cytometry analysis of B1a cells in the spleen and peritoneal cavity.

(B) Comparison of the percentage of B1a cells in the spleen and peritoneal cavity. *p < 0.05; ****p < 0.0001

(C) Purified sera from 4-week-old CBA/N mice shows minimal reactivity to COL7. The yellow arrowheads indicate the bands corresponding to COL7 recognized by serum IgM antibodies. PC, positive control, detected using Anti-DDDDK-tag mAb-HRP-DirecT; NC, negative control, in which PBS was used instead of the primary antibody, followed by peroxidase-conjugated AffiniPure Rabbit Anti-Mouse IgM (μ-chain specific).

Supplementary Figure 1. Comparison of direct immunofluorescence staining with four antibodies in tail skin from 2-year-old mice.



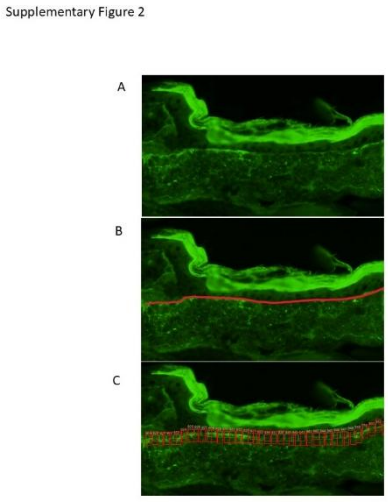
(A) Alexa Fluor 488 AffiniPure Goat Anti-Mouse IgM, µ chain specific (JacksonImmunoresearch, 115-545-020).

(B) Alexa Fluor 488 AffiniPure $F(ab')_2$ Fragment Goat Anti-Mouse IgM, µ chain specific (JacksonImmunoresearch, 115-546-075).

(C) A Goat anti-Mouse IgM (Heavy chain) Cross-Adsorbed Secondary Antibody, Alexa Fluor 488 (Invitrogen, A21042).

(D) Alexa Fluor 488 AffiniPure Rabbit Anti-Mouse IgM, µ chain specific (JacksonImmunoresearch, 315-545-020).

Supplementary Figure 2. How to analyze the deposition at DEJ.



For quantification of the deposition of IgM antibody by ImageJ, the DIF image was visually inspected (A), and a red line was manually drawn along the DEJ (B). Multiple rectangular regions, 10 μm in width and centered on the red line, were defined and used to quantify the Alexa Fluor fluorescence intensity (C).

Supplementary Figure 3. Aged mice do not undergo class switching to IgG after the administration of DPP-4 inhibitors or PD-1 inhibitors.

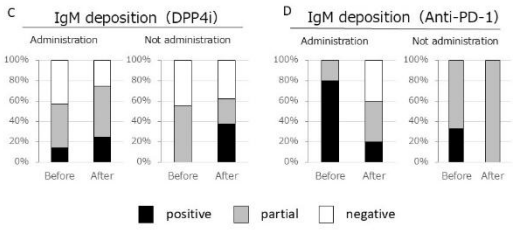
Supplementary Figure 3

A

DPP4i	IgM		IgG		C3	
	Before	4 months later	Before	4 months later	Before	4 months later
+	+	+	−	−	−	−
+	−	±	−	−	−	−
+	−	−	−	−	−	−
+	−	−	−	−	−	−
+	±	+	−	−	−	−
+	±	±	−	−	−	−
+	±	±	−	−	−	+
−	±	±	−	−	−	−
−	−	+	−	−	−	−
−	±	+	−	−	−	−
−	−	−	−	−	−	−
−	−	±	−	−	−	−
−	+	+	−	−	−	±
−	±	−	−	−	−	−
−	−	+	−	−	−	−
−	±	−	−	−	−	−

B

Anti-PD-1	IgM		IgG		C3	
	Before	4 months later	Before	4 months later	Before	4 months later
+	+	−	+	−	−	−
+	+	+	−	−	−	−
+	+	±	−	−	+	−
+	±	−	−	−	−	−
+	+	+	−	−	−	−
iso	±	±	−	−	±	−
iso	±	±	−	−	−	−
iso	+	±	+	+	±	−

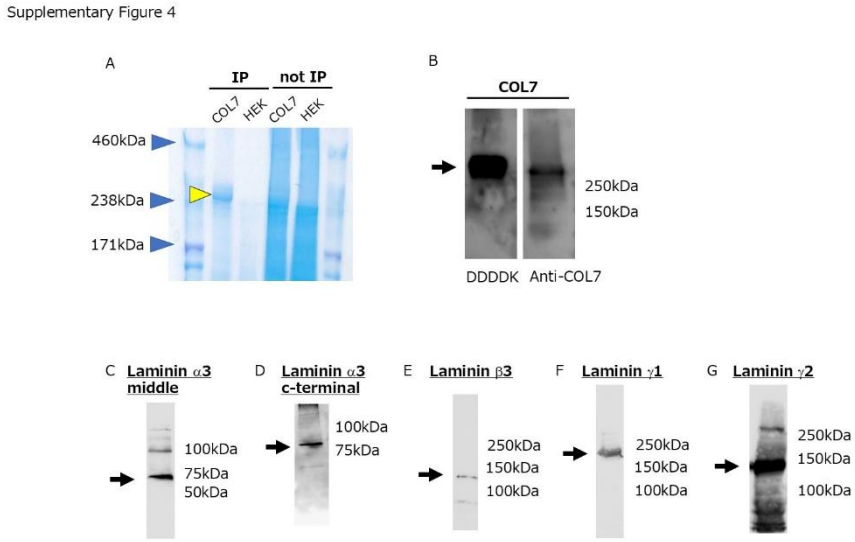


(A) The result of deposition of IgM, IgG and C3 before and after the administration of DPP-4 inhibitors.

(B) The result of deposition of IgM, IgG and C3 before and after the administration of PD-1 inhibitors.

(C, D) The bar graph of IgM deposition.

Supplementary Figure 4. Confirming recombinant proteins



(A) Coomassie Brilliant Blue staining of immunoprecipitated (IP) DDDDK-COL7 shows a 290-kDa band (yellow arrowhead).

(B) Western blotting of DDDDK-COL7 using anti-DDDDK antibody (left) and anti-COL7 antibody (right).

(C) Western blotting of DDDDK- Laminin α3 middle using anti-DDDDK antibody.

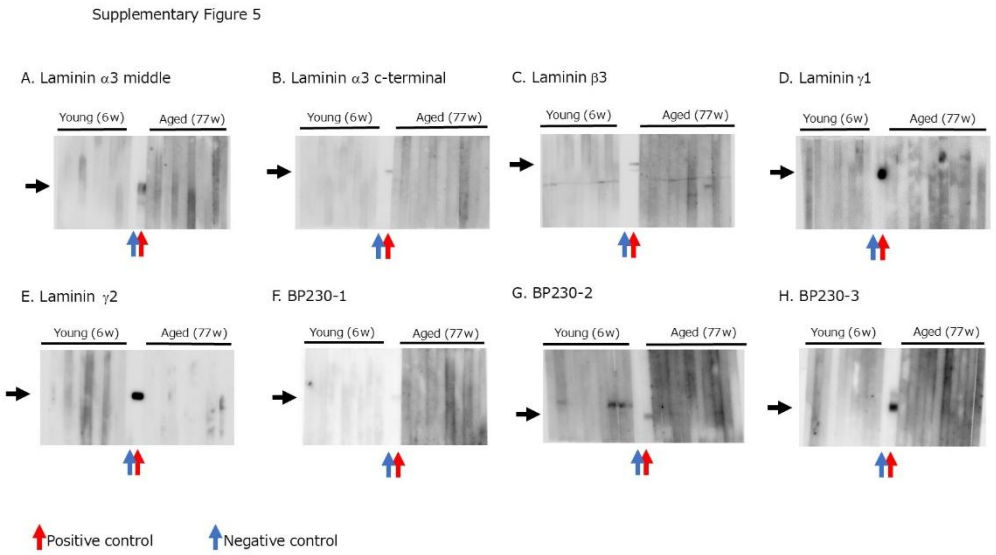
(D) Western blotting of DDDDK- Laminin α3 c-terminal using anti-DDDDK antibody.

(E) Western blotting of Laminin β3 using anti-mouse Laminin β3.

(F) Western blotting of Laminin γ1 using anti-mouse Laminin γ1.

(G) Western blotting of Laminin γ2 using anti-mouse Laminin γ2.

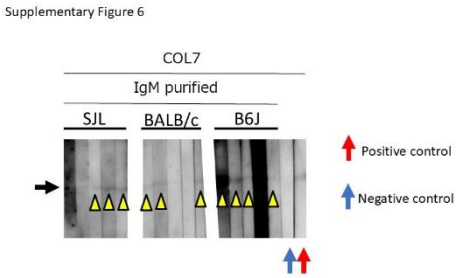
Supplementary Figure 5. None of the aged mice sera reacts with the recombinant proteins as below.



Immunoblotting of young mice sera (6-week-old) and aged mice sera (77-week-old) with Laminin α3 middle (A), Laminin α3 c-terminal (B), Laminin β3 (C), Laminin γ1 (D), Laminin γ2 (E), BP230-1 (F), BP230-2 (G) and BP230-3 (H). (n = 10 per group)

PC, positive control, detected using Anti-DDDDK-tag mAb-HRP-DirecT; NC, negative control, in which PBS was used instead of the primary antibody, followed by peroxidase-conjugated AffiniPure Rabbit Anti-Mouse IgM (μ-chain specific).

Supplementary Figure 6. Anti-COL7 IgM is intrinsically produced regardless of strains.



Purified sera from 3/5 4-week-old SJL mice, 3/5 4-week-old BALB/c mice and 4/5 4-week-old B6J mice react against COL7. The yellow arrowheads indicate the bands corresponding to COL7 recognized by serum IgM antibodies. PC, positive control, detected using Anti-DDDDK-tag mAb-HRP-DirecT; NC, negative control, in which PBS was used instead of the primary antibody, followed by peroxidase-conjugated AffiniPure Rabbit Anti-Mouse IgM (μ-chain specific).